MicroRNA-485-5p suppresses the progression of esophageal squamous cell carcinoma by targeting flotillin-1 and inhibits the epithelial-mesenchymal transition

RIYANG ZHAO[1], YANAN SHAN[1], XINLIANG ZHOU[2], CONG ZHANG[1], RUINIAN ZHAO[1], LIANMEI ZHAO[1] and BAOEN SHAN[1]

[1]Research Centre, The Fourth Hospital of Hebei Medical University; [2]Department of Oncology, The Fourth Hospital of Hebei Medical University, Shijiazhuang, Hebei 050011, P.R. China

Received October 16, 2020; Accepted February 2, 2021

DOI: 10.3892/or.2021.8044

Abstract. As esophageal squamous cell carcinoma (ESCC) is one of the most frequently diagnosed cancers in Asia, it is crucial to uncover its underlying molecular mechanisms that support its development and progression. Several articles have reported that microRNA (miR)-485-5p inhibits the malignant phenotype in a number of cancer types, such as lung, gastric and breast cancer, but to the best of our knowledge, its function in ESCC has not been studied in depth until the present study. It is of great significance to probe the regulatory action and underlying mechanism of miR-485-5p in ESCC. In brief, this study identified that miR-485-5p expression in ESCC tissues was significantly lower than that in normal tissues. The decrease in miR-485-5p expression was associated with a larger tumour size and poor histology and stage. The expression of miR-485-5p was relatively high in Eca 109 and TE-1 cells, but relatively low in KYSE 30. The overexpression of miR-485-5p inhibited cell proliferation, migration and invasion *in vitro*, whereas miR-485-5p knockdown did the opposite. Flotillin-1 (FLOT-1) can facilitate the malignant phenotype in various cancer types. The present study found that in ESCC tissue, the protein expression of FLOT-1 was negatively correlated with miR-485-5p expression. Further experiments showed that miR-485-5p directly targeted the 3'-untranslated region of FLOT-1. The overexpression of miR-485-5p significantly suppressed the mRNA and protein expression levels of FLOT-1, whereas knockdown had the reverse effects. Furthermore, overexpression of miR-485-5p restrained epithelial-mesenchymal metastasis (EMT)-related factors at both the mRNA and protein levels. At the same time, it also inhibited the growth of ESCC and restrained the EMT *in vivo*. In summary, miR-485-5p was found to be an inhibitor of ESCC and may have potential as a novel target candidate for ESCC treatment.

Introduction

Cancer is anticipated to be the leading cause of death worldwide in the 21st century and is expected to be the main barrier to increasing life expectancy (1). Esophageal cancer (EC) ranks seventh according to incidence (572,000 new cases), and sixth in terms of mortality (509,000 deaths) (1), while it ranks third (477,900 new cases) and fourth (375,000 deaths) in terms of incidence and mortality in China (2). EC primarily consists of two cell types, esophageal squamous cell carcinoma (ESCC) in addition to esophageal adenocarcinoma. ESCC is the most common (90%) histological subtype of EC (3); ~70% of cases occur in men (1). Over the past decade, the early stage detection and overall survival rates have improved, benefiting from the increased uptake of early referral schemes, novel endoscopic therapies and perioperative treatment strategies in some developed countries. However, the overall survival among patients with EC remains low; the 5-year survival is 10-15% among all patients, although it increases to 40% among patients who undergo curative surgery (4,5). Therefore, the molecular mechanism of EC underlying its development and progression is of great significance.

It is commonly known that the microRNA (miRNA/miR) family, which are composed of 18-25-nucleotide short non-coding RNAs, can regulate the expression of target mRNAs by binding to the 3'-untranslated regions (3'-UTRs). These miRNAs can downregulate the expression of target mRNA, which negatively modulates the gene expression or mRNA degradation at the posttranscriptional level (6-8). For example, miR-1254 downregulates E3 ubiquitin-protein ligase SMURF1 to reduce cell proliferation, migration and Matrigel

Correspondence to: Professor Baoen Shan, Research Centre, The Fourth Hospital of Hebei Medical University, 12 Jiankang Road, Shijiazhuang, Hebei 050011, P.R. China
E-mail: shanbaoen@163.com

Abbreviations: ESCC, esophageal squamous cell carcinoma; miRNA, microRNA; 3'UTR, 3'untranslated region; NC, negative control; FLOT-1, flotillin-1; RT-qPCR, reverse transcription-quantitative PCR; EMT, epithelial-mesenchymal transition

Key words: esophageal squamous cell carcinoma, expression, miR-485-5p, FLOT-1, clinicopathological features

invasion in gastric cancer cell lines (9), while miRNA-146a downregulates VEGF to reduce cancer metastasis in hepatocellular carcinoma (10). To date, miRNAs have been regarded as vital factors in cancer progression, including tumour proliferation, migration, invasion, metastasis and radiosensitivity (11-15). It has been found that miR-485-5p, which regulates different targets in various human cancers, has the ability to function as a suppressor tumour gene. miR-485-5p downregulates the expression of tumour protein D54 (16) and paired box 3 (17) to inhibit the proliferation and invasion of glioma cells. However it can also reduce the O-GlcNAcylation of polycomb complex protein BMI-1 (18) and inhibit proliferation by targeting CD147 in colorectal cancer (19). Han *et al* (20) reported that O-linked N-acetylglucosamine transferase could be downregulated by the tumour suppressor miR-485-5p to inhibit the progression of ESCC, while in the present study another target was found, flotillin-1 (FLOT-1).

Flotillins are a group of ubiquitously expressed, evolutionarily conserved, membrane-associated scaffolding proteins located on microdomain lipid rafts containing two homologous isoforms, FLOT-1 and FLOT-2, which are involved in various procedures, including cell proliferation, migration, cell adhesion, survival, differentiation, endocytosis, signal transduction, membrane trafficking and T-cell activation (21-27).

In the present study, it was verified that miR-485-5p expression was reduced in ESCC. Cell proliferation, locomotion, invasion and epithelial-mesenchymal metastasis (EMT) were blocked by the overexpression of miR-485-5p. As FLOT-1 is a direct target of miR-485-5p, and various reports have verified FLOT-1 plays an important role in promoting cancer progression (21-27), it was concluded that miR-485-5p suppresses ESCC by targeting FLOT-1 and inhibiting the EMT.

Materials and methods

Subjects and tissue specimens. The Ethics Committee of The Fourth Hospital of Hebei Medical University (Shijiazhuang, China) approved this study (approval no. 2019053). Written informed consent was obtained from all subjects or guardians. In this study, ESCC and adjacent tissues (>1 cm away from the edge of the tumor) were surgically excised from 80 patients with ESCC between August 2015 and August 2018. None of the patients had previously received chemo- or radiotherapy. After surgery, the samples were dipped in RNAlater™ (Ambion; Thermo Fisher Scientific, Inc.) and stored in a -80˚C freezer immediately for further use. The specimens were clinically and histologically diagnosed by the Department of Thoracic Surgery and Pathology, The Fourth Hospital of Hebei Medical University. The lymph node metastasis and staging of patients was determined according to The AJCC Esophageal Cancer Staging System, Eighth Edition (28).

Cell lines and culture. ESCC cell lines Eca 109, KYSE 170, KYSE 180 and TE-1 were obtained from the Shanghai Institutes for Biological Sciences. KYSE 30, KYSE 510, TE-12 and YES-2 cell lines were provided by Professor Masatoshi Tagawa (Department of Molecular Biology and Cancer Biology, Chiba University, Chiba, Japan). All cells were cultured in air containing 5% CO_2 at 37˚C in RPMI-1640 medium (Gibco; Thermo Fisher Scientific, Inc.) supplemented with 10% fetal bovine serum (Biological Industries), 1% penicillin and streptomycin (Invitrogen; Thermo Fisher Scientific, Inc.).

Transfection. KYSE 30, Eca 109 and TE-1 cell lines (at 70% density), were transfected with 100 nM miR-485-5p mimics (cat. no. miR10002175-1-5; Guangzhou RiboBio Co., Ltd.), miRNA mimic negative controls (mimics-NC; cat. no. miR1N0000001-1-5; Guangzhou RiboBio Co., Ltd.), miR-485-5p inhibitor (cat. no. miR20002175-1-5; Guangzhou RiboBio Co., Ltd.), miRNA inhibitor negative controls (inhibitor-NC; cat. no. miR2N0000001-1-5; Guangzhou RiboBio Co., Ltd.), FLOT-1 plasmid (2 μg/well; YouBio) and pcDNA 3.1 (2 μg/well; YouBio) using Lipofectamine® 2000 (Invitrogen; Thermo Fisher Scientific, Inc.), according to the manufacturer's instructions. The time interval between transfection and subsequent experimentation was 48 h.

RNA extraction and reverse transcription-quantitative (RT-q)PCR. According to the protocols reported previously (29), RNA extraction and RT-qPCR were carried out. Total RNA was extracted from cells or tissues using TRIzol reagent (Invitrogen; Thermo Fisher Scientific, Inc.). According to the manufacturers' instructions, the GoScript™ Reverse Transcription System (Promega Corporation) was used to synthesize cDNA from 2 μg total RNA It is worth noting that the reverse transcription primer of U6 and miR-485-5p replacing random primer were used to perform target-specific reverse transcription. Meanwhile, cDNA, which was used to quantitate the expression of mRNA, was reverse transcribed as described previously (29). qPCR was performed in triplicate with a 1:4 dilution of cDNA using the SYBR-Green PCR Kit (Promega Corporation) with the 7500 Real-Time PCR System (Applied Biosystems; Thermo Fisher Scientific, Inc.). The thermocycling conditions were as follows: Initial denaturation at 95˚C for 2 min, followed by 40 cycles of denaturation at 95˚C for 15 sec, and annealing and extension at 60˚C for 1 min. Gene specific qPCR primers were as follows: U6 snRNA reverse transcription primer, 5'-CGCTTCACGAATTTGCGTGTCAT-3'; U6 snRNA forward, 5'-GCTTCGGCAGCACATATACTAAAAT-3' and reverse, 5'-CGCTTCACGAATTTGCGTGTCAT-3'; miR-485-5p reverse transcription primer, 5'-GTCGTATCCAGTGCGTGTCGTGGAGTCGGCAATTGCACTGGATACGACGAATTCA-3'; miR-485-5p forward, 5'-GGAGAGGCTGGCCGTGAT-3' and reverse, 5'-CAGTGCGTGTCGTGGAGT-3'; N-cadherin forward, 5'-TGTTTGACTATGAAGGCAGTGG-3' and reverse, 5'-TCAGTCATCACCTCCACCAT-3'; E-cadherin forward, 5'-CCGCCGGCGTCTGTAGGAA-3' and reverse, 5'-AGGGCTCTTTGACCACCGCTCTC-3'; Vimentin forward, 5'-GAGAACTTTGCCGTTGAAGC-3' and reverse, 5'-TCCAGCAGCTTCCTGTAGGT-3'; zinc finger E-box-binding homeobox 1 (ZEB1) forward, 5'-TTGTAGCGACTGGATTTT-3' and reverse, 5'-AGACGATAGTTGGGTCCCGGC-3'; FLOT-1 forward, 5'-CCCATCTCAGTCACTGGCATT-3' and reverse, 5'-CCGCCAACATCTCCTTGTTC-3'; and GAPDH forward, 5'-GGACCTGACCTGCCGTCTAG-3' and reverse, 5'-GTAGCCCAGGATGCCCTTGA-3'.

All primers were purchased from Generay Biotech Co., Ltd. The relative expression levels of miRNA and mRNA were normalized to U6 and GAPDH expression, respectively. The

relative mRNA expression levels were calculated using the $2^{-\Delta\Delta Ct}$ method (30).

Semi-quantitative PCR. After RNA extraction from ESCC cell lines and target-specific reverse transcription to cDNA, as aforementioned, cDNA was diluted with nuclear free water with a 1:4 dilution. qPCR was performed with the diluted cDNA using the GoTaq® G2 Master Mixes (cat. no. M7822; Promega Corporation) with the GeneAmp™ PCR System 9700 (Applied Biosystems; Thermo Fisher Scientific, Inc.). The thermocycling conditions were as follows: Initial denaturation at 95˚C for 5 min; followed by 35 cycles of denaturation at 95˚C for 15 sec, annealing at 60˚C for 30 sec and extension at 72˚C for 30 sec; and a final extension at 72˚C for 15 min. The agarose gels were 2% with 0.01% ethidium bromide. The gels were visualized using GBOX EF2 gel doc system (Syngene). Sequences of reverse transcription, forward and reverse primers were the same as aforementioned for RT-qPCR.

Cell proliferation assay. After cell transfection with miR-485-5p mimics, mimics-NC, miR-485-5p inhibitor and inhibitor-NC for 24 h, an MTS assay (Promega Corporation) was performed to examine proliferation. Harvesting and subculturing of KYSE 30, Eca 109 and TE-1 cells in 96-well plates (2,500 cells/well) were then performed. Cells were incubated for 0, 24, 48, 72 and 96 h, and cell proliferation was assessed using the MTS assay at each desired time point according to the manufacturer's instructions. MTS reagent (20 μl/well) was added into each well and cells were incubated at 37˚C for 2 h in the dark, and the absorbance was measured at 492 nm by a microplate reader. The experiment was performed in triplicate.

Cell migration and invasion assays. Cell migration and invasion were assessed by migration and invasion assays in a Transwell chamber (Corning, Inc.). Matrigel was used to coat the upper Transwell insert of the chamber at 37˚C overnight in the cell invasion assay. According to the manufacturer's instructions, transiently transfected cells were serum-starved for 2 h in RPMI-1640 without FBS, and $5x10^4$ cells (Eca 109, KYSE 30 and TE-1) were suspended in 200 μl serum-free RPMI-1640 and seeded onto a Transwell insert. RPMI-1640 containing 20% FBS, as a chemoattractant, was added to the Transwell insert below. The cells in the upper chamber migrated to the lower chamber when cultured in humidified air containing 5% CO_2 at 37˚C for 10 h. Then, cells were fixed with 4% paraformaldehyde for 10-15 min and stained with 0.1% crystal violet for 5-10 min at 25˚C. A total of three medium magnification fields (magnification, x200; light microscope) were randomly selected, and the number of migrated or invasive cells was counted. The experiments above were performed in triplicate.

Wound healing assay. Wound healing assays were performed to assess the migratory ability of cells. ESCC cell lines ($5x10^5$) transfected with miR-485-5p mimics or vector were seeded in 6-well plates (at 100% confluency). Linear wounds were scratched using a 200-μl sterile pipette tips when all wells were filled with cells. To remove suspended cells, plates were washed several times with PBS, and the cells were cultured in humidified air containing 5% CO_2 at 37˚C with serum-free RPMI-1640. The wounds were imaged using a light microscope at the same location at 0, 12 and 24 h, and the percentage of the wound area was calculated (wound area/total area). The experiment was carried out three times.

Immunohistochemistry (IHC). All specimens (5 μm) were fixed in 4% formalin at 25˚C for 24 h, and then embedded in paraffin. Antigen retrieval was achieved by boiling the specimen in Tris-EDTA buffer (cat. no. C1038; Beijing Solarbio Science & Technology Co., Ltd.) at 120˚C for 3 min, followed by blocking endogenous peroxide and protein activity with endogenous peroxidase blocker (reagent I, streptavidin-avidin-biotin detection system; cat. no. SP-9001, ZSGB-BIO) for 20 min in the dark at 25˚C. After blocking with normal goat serum (reagent II, streptavidin-avidin-biotin detection system; cat. no. SP-9001, ZSGB-BIO) at 25˚C for 30 min, sections were incubated with primary antibodies specific for FLOT-1 (1:100; cat. no. 18634; Cell Signaling Technology, Inc.), E-cadherin (1:100; cat. no. ab40772; Abcam), Ki-67 (1:100; cat. no. 27309-1-AP; ProteinTech Group, Inc.), N-cadherin (1:50; cat. no. 22018-1-AP; ProteinTech Group, Inc.) and Vimentin (1:100; cat. no. 10366-1-AP; ProteinTech Group, Inc.) overnight at 4˚C, Next, sections were incubated with the secondary antibody (reagent III, streptavidin-avidin-biotin detection system; cat. no. SP-9001, ZSGB-BIO) at 37˚C for 30 min, followed by incubation with a HRP-labelled streptavidin solution (reagent IV, streptavidin-avidin-biotin detection system; cat. no. SP-9001, ZSGB-BIO) at 25˚C for 30 min. Sections were washed with PBS after each step. After visualization of the positive antigen antibody reaction by incubation with 3,3-diaminobenzidine-tetrachloride (DAB, cat. no. ZLI-9018; ZSGB-BIO) at 25˚C for 5 min, sections were counterstained with haematoxylin at 25˚C for 3 min and evaluated by light microscopy at x40 and 200 magnification.

The expression of FLOT-1 was evaluated using IHC scores by choosing five views with high power lenses at random. The total number of tumour cells and the number of positive cells were calculated. The percentage of positive cells in the total number of tumour cells was calculated. The corresponding scores of positive cell percentages are shown as follows: i) 0, 0-25% positive cells; ii) 1, 26-50% positive cells; iii) 2, 51~75% positive cells; and iv) 3, 76~100%. In addition to the percentages of positive cells, FLOT-1 expression was also scored according to the dyeing strength: i) 0, no claybank; ii) 1, light claybank; iii) 2, medium claybank; and iv) 3, dark claybank. FLOT-1 expression in tissues was ranked according to the following scores: i) 0, -; ii) 1-2, +; iii) 3-4, ++; and iv) 5-6, +++. All the sections were interpreted by two pathologists.

Dual-luciferase reporter assay. TargetScan (http://www.targetscan.org/vert_72/) was employed to predict the targets of miR-485-5p. The FLOT-1 mRNA 3'-UTR target sequence was cloned by Creative Biogene. The wild-type (WT) or mutant (MUT) miR-485-5p binding sequence of FLOT-1 was inserted into the pmirGLO plasmid (YouBio) to establish the recombinant luciferase reporter plasmids (FLOT-1 WT and FLOT-1 MUT). 293T cells (Procell Life Science & Technology Co., Ltd.) were co-transfected with pmirGLO, FLOT-1 WT

or FLOT-1 MUT and miR-485-5p mimics or mimics-NC with Lipofectamine® 2000. Following 48 h of incubation, the firefly and *Renilla* luciferase activities of 293T cells were examined using the Dual-Luciferase® Reporter Assay System (cat. no. E1910; Promega Corporation) following the manufacturer's protocols. The relative luciferase activity was determined by normalizing the firefly luciferase activity against the *Renilla* luciferase activity.

Western blotting. Total protein was obtained from Eca 109 or KYSE 30 cells using RIPA buffer and PMSF (Beijing Solarbio Science & Technology Co., Ltd.). Protein concentration was determined using a BCA Protein Assay kit (cat. no. SI255483; Pierce; Thermo Fisher Scientific, Inc.). Proteins (80 μg/lane) were separated via SDS-PAGE on 10% gels, and then separated proteins were electrophoretically transferred onto PVDF membranes (EMD Millipore). Membranes were then blocked with 5% skimmed milk at room temperature for 1 h. The membrane was incubated with antibodies against FLOT-1 (1:1,000; cat. no. 18634; Cell Signaling Technology, Inc.), E-cadherin (1:1,000; cat. no. ab40772; Abcam), ZEB1 (1:500; cat. no. 21544-1-AP; ProteinTech Group, Inc.), N-cadherin (1:500; cat. no. 22018-1-AP; ProteinTech Group, Inc.), Vimentin (1:500; cat. no. 10366-1-AP; ProteinTech Group, Inc.) and GAPDH (1:10,000; cat. no. AP0063; Bioworld Technology, Inc.) at 4˚C for 12 h. Next, the membranes were incubated at room temperature for 1 h with a fluorochrome-labelled secondary anti-rabbit IgG (1:10,000; cat. no. 926-32211; LI-COR Biosciences). The membranes were visualized using the Odyssey® Infrared Imaging System (LI-COR Biosciences). GAPDH served as a loading control. Western blot analysis was carried out three times, independently.

Lentiviral transfection. Eca 109 cells were cultured in 6-well plates. HitransG P (40 μl/well; GeneChem, Inc.) together with lentivirus-miR-485-5p (MOI 10) or lentivirus-vector (5 μl/well; GeneChem, Inc.) labeled with enhanced green fluorescent protein (EGFP) were added into the wells. HitransG P and lentivirus-miR-485-5p or lentivirus-vector were removed 12-18 h later. Then, cells were cultured in humidified air containing 5% CO_2 at 37˚C for 72 h. Millesimal puromycin was used to select cells for 24 h. The cells were observed under a fluorescence microscope, if the EGFP-labeled cells were nearly at 100%, the lentiviral transfection was successful.

Tumour xenograft in animals. A total of 12 male athymic Balb/c nude mice (4-6 weeks, 20-25 g) were purchased from Beijing Vital River Laboratory Animal Technology Co., Ltd. All animal experiments were performed with approval from the Animal Care Committee of The Fourth Hospital of Hebei Medical University (approval. no. 110324200104285428). The mice were housed at The Fourth Hospital of Hebei Medical University Experiment Animal Centre (humidity, 50%; temperature, 25˚C; light cycle, 12 h light/12 h dark; *ad libitum* access to food and water). The mice were randomly divided into two groups with six mice per group. Eca 109 cells were stably transfected with lentivirus-miR-485-5p or lentivirus-vector. Cells were suspended in PBS ($5x10^6$ cells/200 μl) and injected into the right flanks of mice subcutaneously. Tumour volumes were monitored with a calliper every 5 days. Following which, the mice were sacrificed by spinal dislocation on day 32. Finally, the tumours were removed and weighed and fixed in formalin for IHC analysis, as described above.

Statistical analysis. Statistics were calculated using GraphPad Prism (v5.0) software (GraphPad Software, Inc.) and SPSS v22.0 (IBM Corp.). The experimental data are presented as the mean ± standard deviation from at least three separate experiments. For comparison among the paired samples, paired t-tests were performed. For comparison among the unpaired samples, an unpaired Student's t-test was performed. One-way ANOVA followed by Dunnett's post hoc test was used to examine the significant differences in the experimental data between multiple groups. The relationship between clinicopathological results and the expression of miR-485-5p was examined using a Pearson's chi-squared test. The correlation between miR-485-5p and FLOT-1 expression was analysed using Spearman's correlation analysis. $P<0.05$ was considered to indicate a statistically significant difference.

Results

miR-385-5p is downregulated in ESCC tissues. The relative expression of miR-485-5p in 80 pairs of ESCC and paracarcinoma tissues was detected via RT-qPCR. As shown in Fig. 1A, human ESCC tissues exhibited lower expression of miR-485-5p than adjacent control tissues.

It was also demonstrated that the expression of miR-485-5p was strongly associated with the clinicopathological features of ESCC. Based on the expression of miR-485-5p, 80 ESCC samples were split into two groups. There were 44 cases in the high expression group and 36 cases in the low expression group. Decreased miR-485-5p expression was associated with a larger tumour size and poor differentiation and stages III/IV. Moreover, a decrease in miR-485-5p was more common in male patients (Table I). These data indicated that the expression of miR-485-5p was downregulated in ESCC tissues.

Furthermore, the expression of miR-485-5p was examined in ESCC cell lines (KYSE 30, KYSE 170, KYSE 180, KYSE 510, Eca 109, TE-1, TE-12 and YES-2) by semi-quantitative PCR. miR-485-5p expression was verified to be relatively high in Eca 109 and TE-1 cells, but relatively low in KYSE 30 cells, as shown in Fig. 1B. Thus, these three cell lines were used for the following experiments.

KYSE 30, Eca 109 and TE-1 cell lines were transfected with miR-485-5p mimics and inhibitor to explore the role of miR-485-5p in the biological functions of ESCC cells. The ratio of cell line transfection was validated by RT-qPCR. As indicated in Fig. 1C, the expression of miR-485-5p was significantly upregulated in mimics group and downregulated in the inhibitor group, compared with the control groups.

miR-485-5p inhibits the proliferation, migration and invasion of ESCC cell lines. The influence of miR-485-5p on the proliferative capacity of ESCC cells was verified using an MTS assay. Compared with Eca 109, KYSE 30 and TE-1 cells transfected with the inhibitor-NC, the proliferation rates of cells transfected with miR-485-5p inhibitor were increased. Whereas, the inhibition rates of Eca 109, KYSE 30 and TE-1 cells transfected with miR-485-5p mimics were decreased in

Table I. Association between clinicopathological characteristics of patients with esophageal squamous cell carcinoma and miR-485-5p expression.

Clinicopathological characteristics	miR-485-5p expression		P-value
	High	Low	
Age, years			0.369
≥65	24	16	
<65	20	20	
Sex			0.021[a]
Male	36	21	
Female	8	15	
Size, cm^3			0.014[a]
≥10	16	23	
<10	28	13	
Lymph node metastasis			0.805
Present (N1-N3)	22	17	
Absent (N0)	22	19	
Histological type			0.001[b]
Poor	14	25	
Well to moderate	30	11	
Stage			0.006[b]
I/II	27	11	
III/IV	17	25	

[a]P<0.05; [b]P<0.01. miR, microRNA.

contrast to cells transfected with mimics-NC. The proliferation rate was significantly reduced in Eca 109, KYSE 30 and TE-1 cells transfected with miR-485-5p mimics compared with the mimics-NC group, while the opposite effect was observed in the inhibitor group (Fig. 2A).

Further investigation demonstrated the inhibitory role that miR-485-5p played in ESCC cells. The migration ratios of Eca 109, KYSE 30 and TE-1 cells transfected with miR-485-5p mimics were reduced, whereas the migration ratios of Eca 109, KYSE 30 and TE-1 cells transfected with miR-485-5p inhibitor were significantly increased (Fig. 2B and C). Moreover, compared with the negative control, the invasion ratio was also decreased in Eca 109, KYSE 30 and TE-1 cell lines overexpressing miR-485-5p, but increased in the miR-485-5p knockdown group (Fig. 2D and E).

Next, a wound healing assay was performed to confirm these results. Compared with the negative control, the migratory rates of Eca 109, KYSE 30 and TE-1 cells transfected with mimics at 24 h were decreased. The overexpression of miR-485-5p reduced the migratory rate of ESCC cells (Fig. 2F). Additionally, the statistical results uncovered the suppressive role of miR-485-5p in the migration of ESCC cells (Fig. 2G).

FLOT-1 is a predicted target of miR-485-5p. TargetScan (http://www.targetscan.org/vert_72/) was employed to predict targets of miR-485-5p. According to TargetScan, FLOT-1, which is an oncogene related to a number of malignancies (21-27,31), might also be a target gene of miR-485-5p (Fig. 3A). As Guo *et al* (31) verified that the upregulation of FLOT-1 enhanced the malignant phenotype of lung adenocarcinoma cells *in vitro*, including cell proliferation, migration and invasion, it is of significance to explore whether the potential mechanism by which miR-485-5p inhibits ESCC is related to inhibition of the expression of FLOT-1. First, the FLOT-1 plasmid was constructed and transfection efficacy was verified via western blotting (Fig. 3B). Compared with cells transfected with pcDNA3.1, the protein expression of FLOT-1 was increased in cells transfected with the FLOT-1 plasmid. To confirm the predicted result, FLOT-1 expression was determined in ESCC cell lines transfected with miR-485-5p mimics or inhibitor via RT-qPCR and western blotting. Both the mRNA and protein levels were relatively high in cells transfected with the inhibitor, whereas the cells transfected with miR-485-5p mimics showed the opposite effect in comparison with the control group (Fig. 3C and D).

In addition, to further verify whether FLOT-1 is a direct target of miR-485-5p, a dual-luciferase reporter assay system was utilized. MUT and WT FLOT-1 3'UTR (site-directed mutations were contained in the former) were cloned into pmirGLO reporter plasmids. pmirGLO-WT-FLOT-1 3'UTR and miR-485-5p mimics were co-transfected into 293T cells. As shown in Fig. 3E, a notably decreased luciferase activity could be observed in the FLOT-1 WT + miR-485-5p mimics group compared with the FLOT-1 WT + mimics-NC group. Moreover, the overexpression of miR-485-5p did not have any

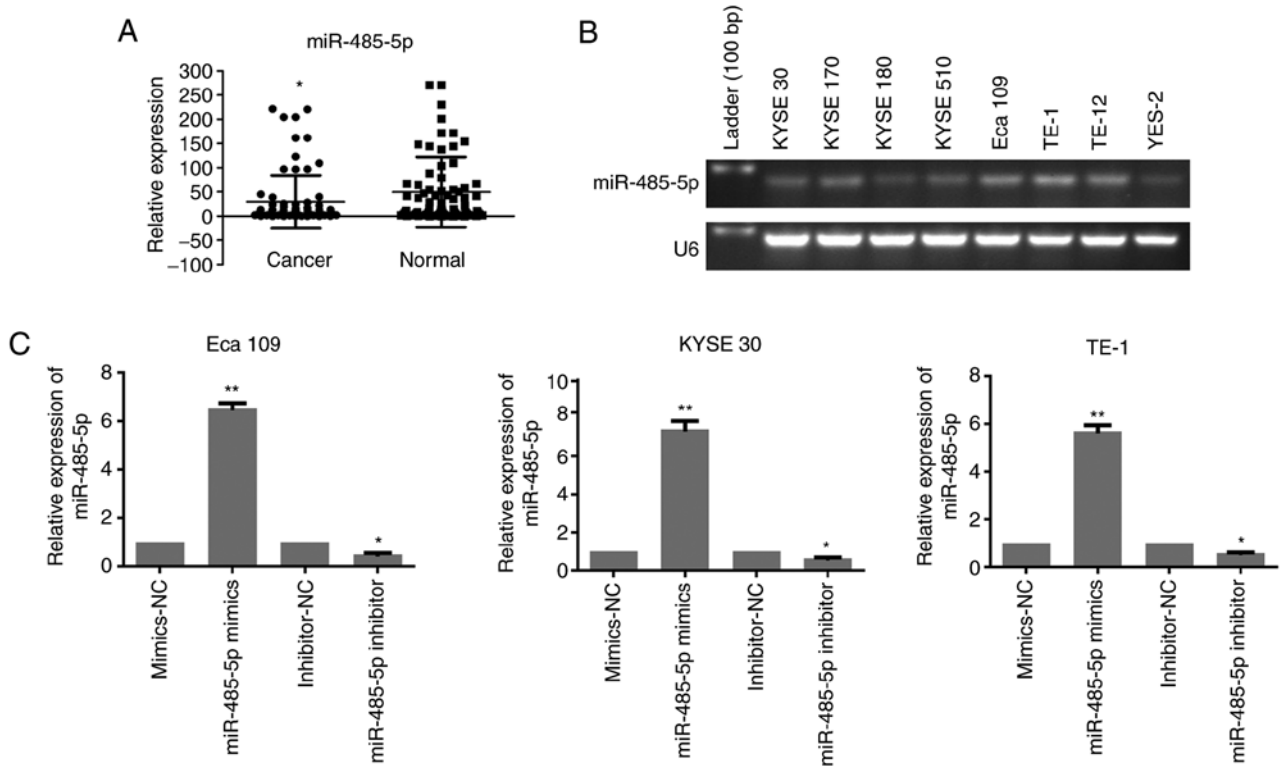

Figure 1. miR-385-5p is downregulated in ESCC tissues. (A) The expression of miR-485-5p in 80 pairs of ESCC and paracarcinoma tissues was detected by RT-qPCR. (B) The expression of miR-485-5p in ESCC cell lines was assessed by PCR. (C) The miR-485-5p transfection efficacy was verified in Eca 109, KYSE 30 and TE-1 cells transfected with miR-485-5p mimics or miR-485-5p inhibitor via RT-qPCR. The data are expressed as the mean ± SD. *P<0.05 and **P<0.01 vs. control group. miR, microRNA; ESCC, esophageal squamous cell carcinoma; RT-qPCR, reverse transcription-quantitative PCR; NC, negative control.

Table II. Negative correlation between miR-485-5p and FLOT-1 protein expression levels using Spearman's correlation analysis. miR-485-5p expression was measured via reverse transcription-quantitative PCR, and FLOT-1 protein levels were measured by IHC.

	miR-485-5p expression			
FLOT-1 expression	High	Low	r-value	P-value
Negative (-/+)	14	5	-0.560	P<0.01
Positive (++/+++)	6	15		

FLOT-1, flotillin-1; miR, microRNA; IHC, immunohistochemistry.

influence on the luciferase activity of cells transfected with pmirGLO-MUT-FLOT-1 3'UTR.

To determine the relationship between the expression of miR-485-5p and FLOT-1 in ESCC, 40 ESCC samples were collected for examination by RT-qPCR and IHC. These 40 samples were divided into two different groups based on the median expression of miR-485-5p: A high expression group and a low expression group. It was found that there was a moderate negative correlation between FLOT-1 expression and miR-485-5p expression (r=-0.560; Fig. 3F and Table II).

To further confirm that miR-485-5p inhibited tumour progression through FLOT-1 inhibition in ESCC, functional recovery experiments were carried out. miR-485-5p mimics and FLOT-1 plasmids, and their NCs, were co-transfected into the Eca 109 and KYSE 30 cells. After transfection, western blotting was performed for each group to determine FLOT-1 expression (Fig. 3G). The FLOT-1 expression levels in Eca 109 and KYSE 30 cells in the miR-485-5p mimics + pcDNA 3.1 group were notably decreased compared with the cells in the mimics-NC + pc DNA3.1 group, whereas the FLOT-1 expression of cells in the miR-485-5p mimics + FLOT-1 group increased compared with cells in the miR-485-5p mimics + pcDNA3.1 group. These results suggested that the 3'UTR of FLOT-1 was a target of miR-485-5p, yet the interaction was abolished in this sequence by point mutations.

Overexpression of miR-485-5p inhibits the EMT. EMT is an important biological process that promotes the invasion and metastasis of cancer cells. It has been reported that miR-485-5p can reverse EMT in non-small cell lung cancer cells (32). As the present study confirmed that miR-485-5p overexpression could inhibit the migration and invasion of ESCC cells, it was of significance to determine the association between miR-485-5p and EMT in ESCC cells by evaluating the mRNA and protein expression levels of EMT-associated factors. The RT-qPCR and western blotting results revealed that E-cadherin expression in Eca 109 and KYSE 30 cells transfected with miR-485-5p mimics was increased, whereas Vimentin, N-cadherin and ZEB1 expression levels were decreased (Fig. 4A-C).

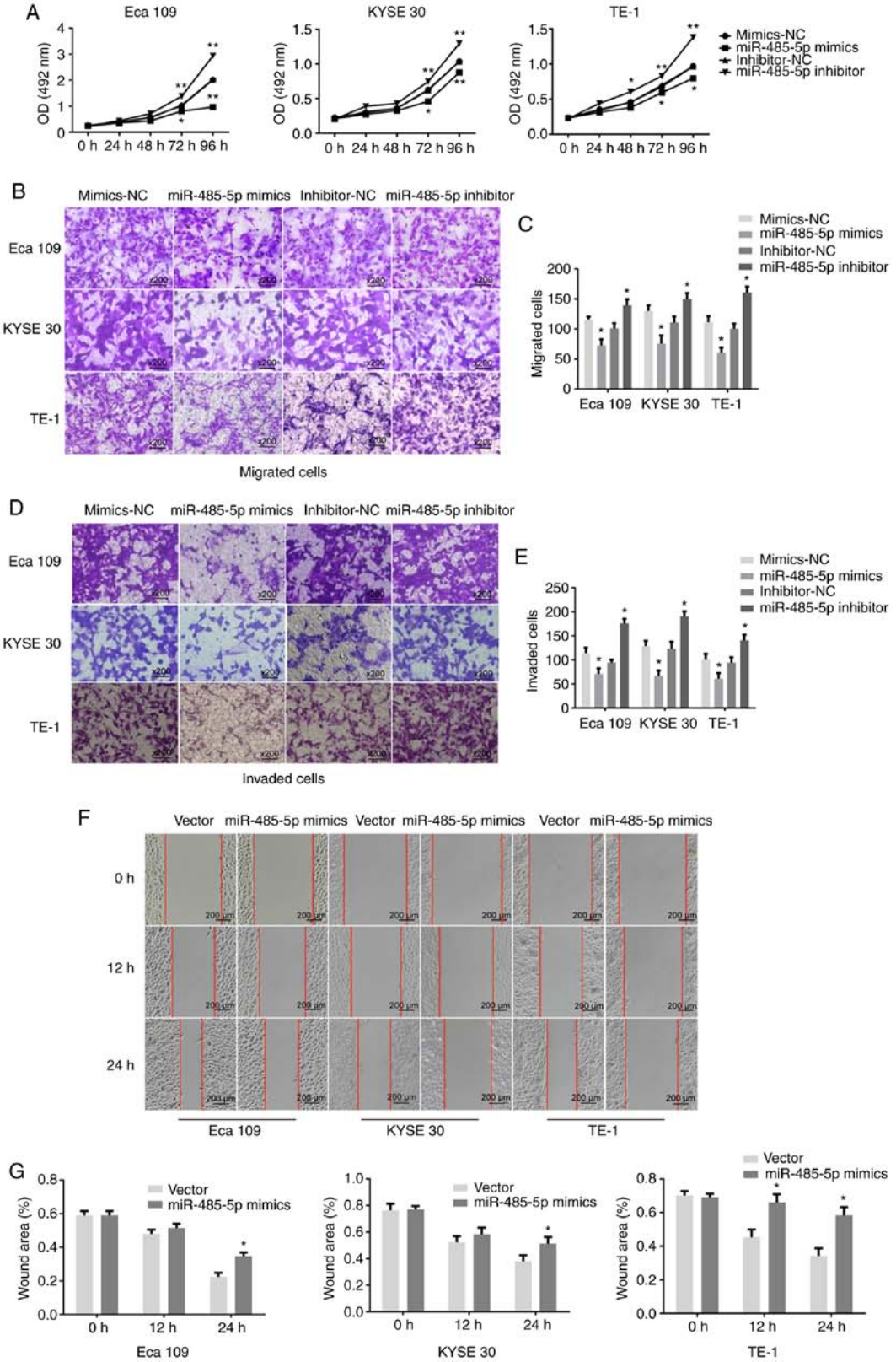

Figure 2. miR-485-5p inhibits the proliferation, migration and invasion of ESCC cell lines. (A) The proliferation of Eca 109, KYSE 30 and TE-1 cells transfected with miR-485-5p mimics or miR-485-5p inhibitor was explored using an MTS assay. (B and D) Cell migration and Matrigel invasion assays (magnification, x200) were performed to detect the effects of miR-485-5p on ESCC cell migration and invasion, and the migratory and invasive abilities were (C and E) quantified as cell numbers. (F) Wound healing assays were performed to detect the migratory ability of cells after transfection with miR-485-5p mimics (scale bar, 200 μm), and (G) the migratory ratio was determined by dividing the wound area by the total area. The data are expressed as the mean ± SD. *P<0.05 and **P<0.01 vs. control group. miR, microRNA; ESCC, esophageal squamous cell carcinoma; NC, negative control.

miR-485-5p suppresses the growth of ESCC in vivo. To illustrate the influence of miR-485-5p on tumour growth *in vivo*, Eca 109 cells transfected with lentivirus-miR-485-5p were injected into the flanks of nude mice, while cells transfected

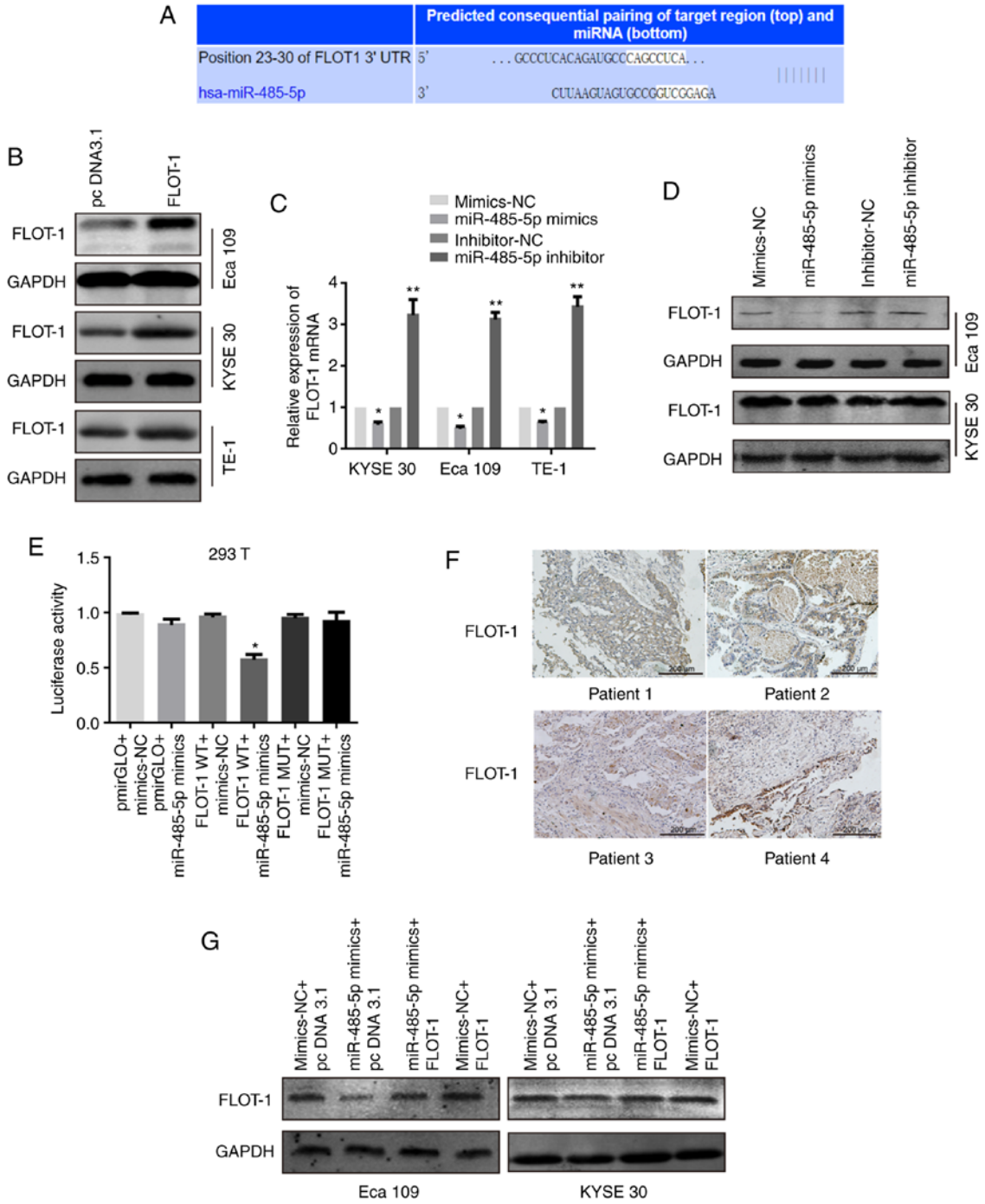

Figure 3. FLOT-1 is a predicted target of miR-485-5p. (A) Bioinformatics analysis predicted a miR-485-5p-binding site in the 3'UTR of FLOT1 mRNA. (B) The FLOT-1 plasmid transfection efficacy was verified in Eca 109, KYSE 30 and TE-1 cells transfected with FLOT-1 plasmid or pcDNA3.1 via western blotting. (C) FLOT-1 mRNA levels in KYSE 30, Eca 109 and TE-1 cells transfected with miR-485-5p mimics, miR-485-5p inhibitor or their corresponding controls (miR-NC and inhibitor-NC). (D) FLOT-1 protein levels of Eca 109 and KYSE 30 cells transfected with miR-485-5p mimics, miR-485-5p inhibitor or their corresponding controls (miR-NC and inhibitor-NC). (E) Effects of miR-485-5p on the translation of the reporter gene inserted downstream of the 3'UTR of FLOT-1 mRNA or the mutated 3'UTR of FLOT-1 mRNA in 293T cells. 293T cells were co-transfected as shown in the figure, and the luciferase activities were measured using a Dual-luciferase reporter assay. The luciferase activity was normalized and expressed as the ratio of firefly/*Renilla* luciferase activities. (F) IHC staining of FLOT-1 expression in esophageal squamous cell carcinoma tissue sections (scale bar, 200 μm). (G) FLOT-1 protein levels in Eca 109 and KYSE 30 cells co-transfected with mimics-NC and pcDNA3.1, miR-485-5p mimics and pcDNA3.1, miR-485-5p mimics and FLOT-1, mimics-NC and FLOT-1. The data are expressed as the mean ± SD. *P<0.05 and **P<0.01 vs. control group. FLOT-1, flotillin-1; miR, microRNA; UTR, untranslated region; NC, negative control; IHC, immunohistochemistry; WT, wild-type; MUT, mutant.

with lentivirus-NC were utilized as the negative control (Fig. 5A and B). As demonstrated in Fig. 5C-E, the lentivirus-miR-485-5p group exhibited an observable decline in tumour volume and weight compared with the control group. On day 32, the volume and weight of tumours transfected with lentivirus-miR-485-5p were 1,324.5±201.39 mm^3 and 0.45±0.11 g, respectively, while those of the negative control were 2,482.83±555.13 mm^3 and 0.76±0.15 g, respectively.

Moreover, the expression levels of FLOT-1, Ki-67 and EMT-related proteins were investigated by IHC. The protein

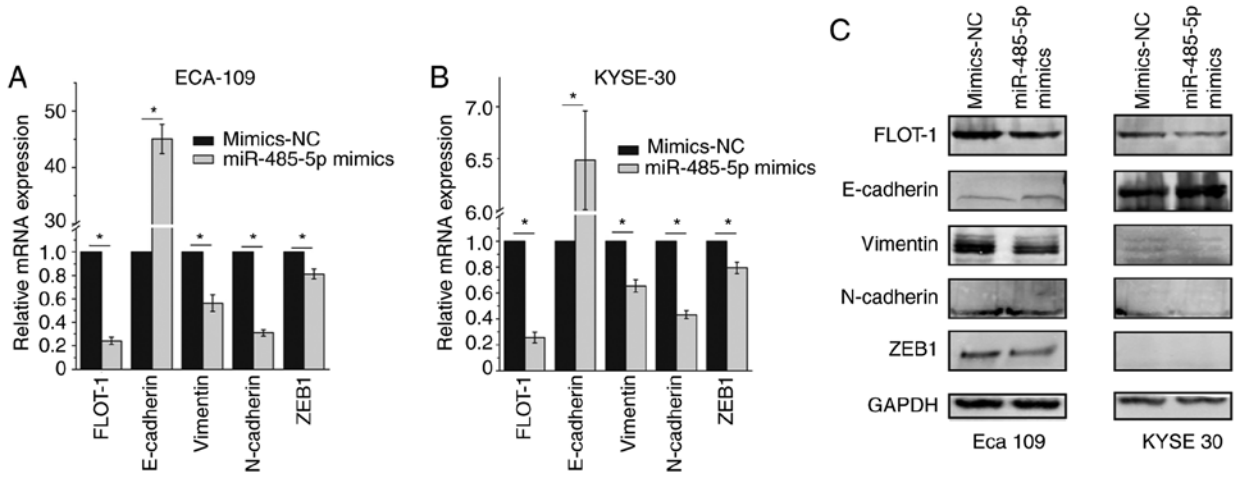

Figure 4. Overexpression of miR-485-5p inhibits the epithelial-mesenchymal transition. The mRNA levels of FLOT-1, E-cadherin, Vimentin, N-cadherin and ZEB1 in (A) Eca 109 and (B) KYSE 30 cells transfected with miR-485-5p or mimics-NC. (C) The protein levels of FLOT-1, E-cadherin, Vimentin, N-cadherin and ZEB1 in Eca 109 (left) and KYSE 30 (right) cells transfected with miR-485-5p or mimics-NC. The data are expressed as the mean ± SD. *P<0.05. FLOT-1, flotillin-1; miR, microRNA; NC, negative control; ZEB1, zinc finger E-box-binding homeobox 1.

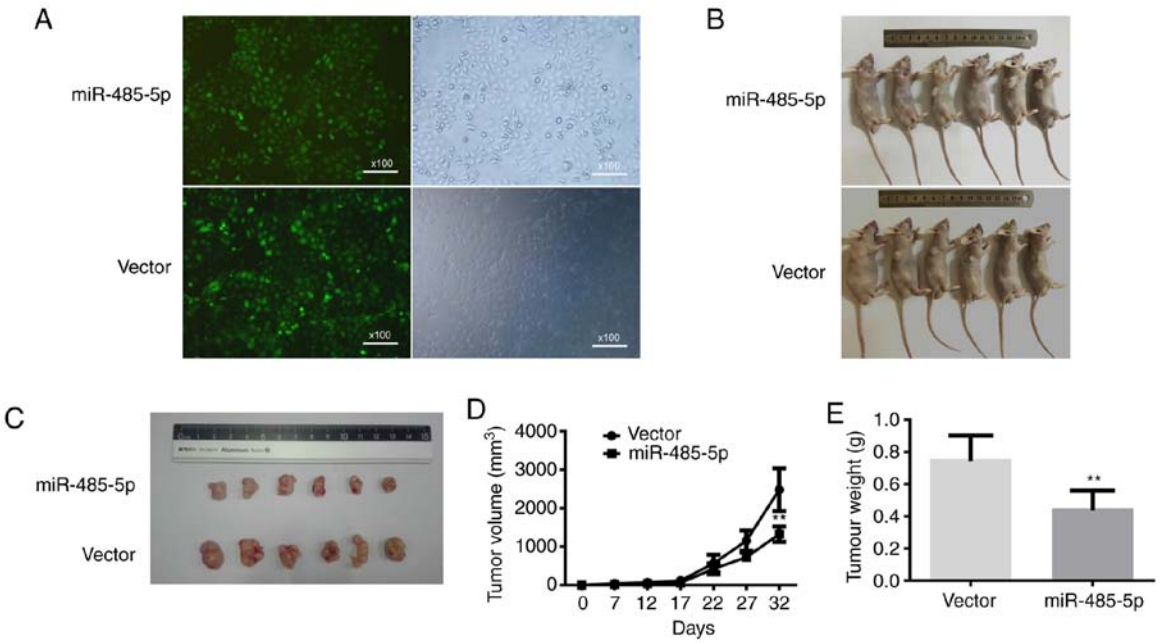

Figure 5. miR-485-5p suppresses the growth of esophageal squamous cell carcinoma *in vivo*. (A) Eca 109 cells transfected with lentivirus-miR-485-5p or lentivirus-NC (magnification, x100). (B) Nude mice were injected into their flanks with Eca 109 cells transfected with lentivirus-miR-485-5p or lentivirus-NC. (C) Eca 109 cells stably expressing miR-485-5p or vector-implanted tumours from nude mice were dissected and imaged after euthanizing the mice. The (D) growth curve and (E) tumour weight of Eca 109 cells stably expressing miR-485-5p or vector implanted tumours from nude mice. n=6 mice per experimental group. **P<0.01 vs. vector group. miR, microRNA; NC, negative control.

expression levels of Ki-67, FLOT-1, N-cadherin and Vimentin, compared with those in the control group, were all obviously decreased in the lentivirus-miR-485-5p transfection group, while E-cadherin was elevated (Fig. 6). In summary, miR-485-5p played roles as a tumour suppressor and apoptosis promotor of ESCC *in vivo*.

Discussion

The first miRNA was discovered in 1993 when the heterochronic gene lin-4 from *Caenorhabditis elegans* was identified as a small non-coding RNA (33). Over the past decades, as an increasing number of miRNAs have been identified, investigators have gradually realized that miRNAs are a cluster of short non-coding RNAs that can inhibit the stability of mRNA structures, decrease the translation ratio of proteins, disrupt the regulation of a number of biological processes, and play a role in cancer development (34). miRNAs have an impact on the biological behaviour of cancer cells, including proliferation, migration, invasion, cell cycle and apoptosis, and play a role in tumour occurrence and development (34-38).

miR-485-5p has been demonstrated to be a functional tumour suppressor. Duan *et al* (39) reported that miR-485-5p functions as a tumour suppressor in gastric cancer by targeting

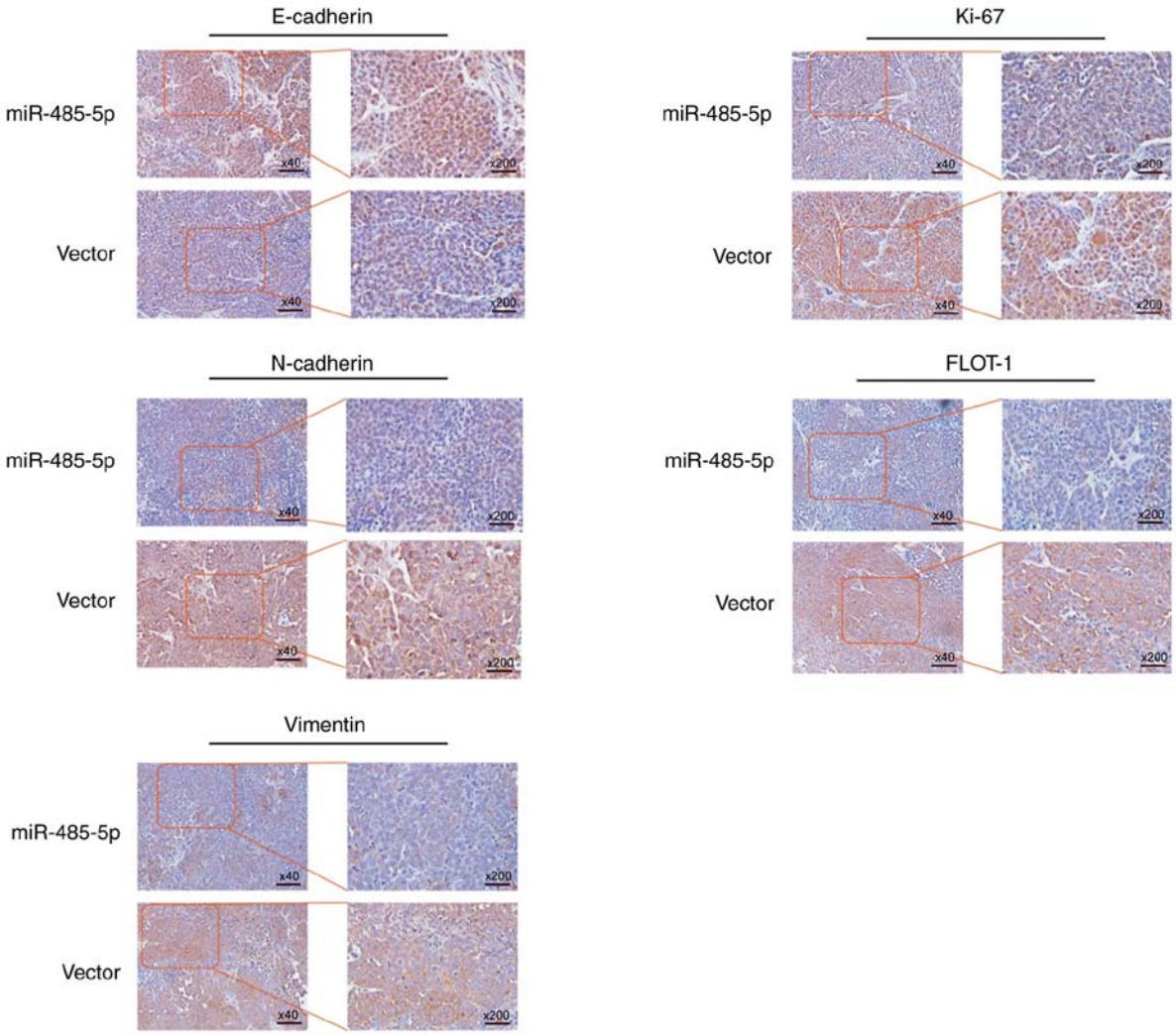

Figure 6. IHC staining of the tissue sections of implanted tumours. IHC staining of E-cadherin, N-cadherin, Vimentin, Ki-67 and FLOT-1 in Eca 109 cells stably expressing miR-485-5p or vector-implanted tumour sections from nude mice (magnification, x40 or 200). n=6 mice per experimental group. IHC, immunohistochemistry; FLOT-1, flotillin-1; miR, microRNA.

7,8-dihydro-8-oxoguanine triphosphatase. Gao *et al* (40) discovered that miR-485-5p blocks the WW domain-binding protein 2/Wnt signalling pathway to inhibit the progression of hepatocellular carcinoma. The inhibitory function of miR-485-5p has also been reported in thyroid cancer (41,42), cholangiocarcinoma (43), lung cancer (32,44), osteosarcoma (45), breast cancer (46) and EC (20). Han *et al* (20) discovered that miR-485-5p, which can downregulate the expression of O-linked N-acetylglucosamine transferase, represses the proliferation and invasion of EC cells. The present study showed that miR-485-5p was reduced in human ESCC, and that overexpression of miR-485-5p could suppress the proliferation, migration and invasion of ESCC cell lines. Through bioinformatics prediction, FLOT-1 was identified as a potential target of miR-485-5p.

Previous studies have revealed that the dysregulation of FLOT is involved in various cancers. Several reports have demonstrated that the overexpression of FLOT-1 increases the ratio of tumourigenicity as well as cell proliferation by activating FOXO3a transcriptional activity in breast cancer (47), whereas the upregulation of FLOT-1 adjusted by NF-κB and Wnt/β-catenin promotes cell invasion, motility and lymph metastasis of the pelvis in cervical carcinoma (48). Furthermore, Liu *et al* (49) verified that highly expressed FLOT-2 facilitates proliferation, migration and invasion in melanoma. Studies have found that FLOT-1 facilitates the signalling of tumour necrosis factor-α (TNF-α) receptor and is relevant to ESCC progression (50). Guo *et al* (31) verified that FLOT-1 promotes the malignant phenotype of lung adenocarcinoma *in vitro*, including cell proliferation, migration and invasion. Moreover, Jang *et al* (51) reported that the sumoylation of FLOT-1 promotes EMT in metastatic prostate cancer.

Previous studies have verified that FLOT-1 facilitates malignant phenotypes, such as cell proliferation, migration, invasion and EMT *in vitro*, while in the present study, the results of bioinformatics prediction showed that FLOT-1 could be a potential target of miR-485-5p. It was verified that the expression of FLOT-1 could be directly reduced by the upregulation of miR-485-5p in ESCC. As shown in the present study, miR-485-5p overexpression inhibited cell proliferation, migration, invasion and EMT in ESCC, thus it is reasonable to conclude that miR-485-5p can inhibit these cell behaviours by repressing FLOT-1 expression. There are some limitations in this article. It was verified that miR-485-5p expression was

higher in ESCC tissues than that in paracancerous tissues, however miR-485-5p expression levels in ESCC cell lines were not compared with a normal esophagus cell line. Although other studies reported FLOT-1 facilitates malignant phenotypes in various cancer types, the present study did not verify its functions in ESCC directly. Overall, understanding the underlying actions of miR-485-5p in the pathogenesis of ESCC will increase the knowledge of the biological basis of tumour progression, which will increase the possibility of developing a novel diagnostic marker and original therapeutic strategy for ESCC.

Acknowledgements

Not applicable.

Funding

This project was supported by the National Natural Science Foundation of China (grant nos. 81973520 and 81673642).

Availability of data and materials

All data generated or analysed during this study are included in this published article.

Authors' contributions

RiZ and YS conceived the hypothesis, designed and performed the experiments. XZ and RuZ conducted the data collection, analysis and interpretation, and wrote the manuscript. CZ collected the specimens, performed the *in vitro* experiments and edited the manuscript. LZ and BS performed the animal experiments, treated the animals, supervised the findings of this work, aided in interpreting the results, and provided the funds and critical revision of the manuscript. YS and LZ confirm the authenticity of all the raw data. All authors read and approved the final manuscript.

Ethics approval and consent to participate

This project was approved by the Ethics Committee of the Fourth Hospital of Hebei Medical University (Shijiazhuang, China). Written informed consent was obtained from all subjects or guardians.

Patient consent for publication

Not applicable.

Competing interests

The authors declare that they have no competing interests.

References

1. Bray F, Ferlay J, Soerjomataram I, Siegel RL, Torre LA and Jemal A: Global cancer statistics 2018: GLOBOCAN estimates of incidence and mortality worldwide for 36 cancers in 185 countries. CA Cancer J Clin 68: 394-424, 2018.
2. Chen W, Zheng R, Baade PD, Zhang S, Zeng H, Bray F, Jemal A, Yu XQ and He J: Cancer statistics in China, 2015. CA Cancer J Clin 66: 115-132, 2016.
3. Brock MV, Gou M, Akiyama Y, Muller A, Wu TT, Montgomery E, Deasel M, Germonpré P, Rubinson L, Heitmiller RF, *et al*: Prognostic importance of promoter hypermethylation of multiple genes in esophageal adenocarcinoma. Clin Cancer Res 9: 2912-2919, 2003.
4. Thrumurthy SG, Chaudry MA, Thrumurthy SSD and Mughal M: Oesophageal cancer: Risks, prevention, and diagnosis. BMJ 366: 14373, 2019.
5. Mariette C, Markar SR, Dabakuyo-Yonli TS, Meunier B, Pezet D, Collet D, D'Journo XB, Brigand C, Perniceni T, Carrère N, *et al*: Hybrid minimally invasive esophagectomy for esophageal cancer. N Engl J Med 380: 152-162, 2019.
6. Bartel DP: MicroRNAs: Genomics, biogenesis, mechanism, and function. Cell 116: 281-297, 2004.
7. He L and Hannon GJ: MicroRNAs: Small RNAs with a big role in gene regulation. Nat Rev Genet 5: 522-531, 2004.
8. Calin GA and Croce CM: MicroRNA signatures in human cancers. Nat Rev Cancer 6: 857-866, 2006.
9. Jiang M, Shi L, Yang C, Ge Y, Lin L, Fan H, He Y, Zhang D, Miao Y and Yang L: MiR-1254 inhibits cell proliferation, migration, and invasion by down-regulating Smurf1 in gastric cancer. Cell Death Dis 10: 32, 2019.
10. Zhang Z, Zhang Y, Sun XX, Ma X and Chen ZN: MicroRNA-146a inhibits cancer metastasis by downregulating VEGF through dual pathways in hepatocellular carcinoma. Mol Cancer 14: 1186, 2015.
11. Garzon R, Calin GA and Croce CM: MicroRNAs in cancer. Annu Rev Med 60: 167-179, 2009.
12. Troschel FM, Böhly N, Borrmann K, Braun T, Schwickert A, Kiesel L, Eich HT, Götte M and Greve B: MiR-142-3p attenuates breast cancer stem cell characteristics and decreases radioresistance in vitro. Tumour Biol 40: 1010428318791887, 2018.
13. Wu Y, Huang J, Xu H and Gong Z: Over-Expression of miR-15a-3p enhances the radiosensitivity of cervical cancer by targeting tumor protein D52. Biomed Pharmacother 105: 1325-1334, 2018.
14. Shao Y, Zhang D, Li X, Yang J, Chen L, Ning Z, Xu Y, Deng G, Tao M, Zhu Y and Jiang J: MicroRNA-203 increases cell radiosensitivity via directly targeting Bmi-1 in hepatocellular carcinoma. Mol Pharm 15: 3205-3215, 2018.
15. Wang L, Peng X, Lu X, Wei Q, Chen M and Liu L: Inhibition of hsa_circ_0001313 (circCCDC66) induction enhances the radio-sensitivity of colon cancer cells via tumor suppressor miR-338-3p: Effects of cicr_0001313 on colon cancer radio-sensitivity. Pathol Res Pract 215: 689-696, 2019.
16. Yu J, Wu SW and Wu WP: A tumor-suppressive microRNA, miRNA-485-5p, inhibits glioma cell proliferation and invasion by down-regulating TPD52L2. Am J Transl Res 9: 3336-3344, 2017.
17. Wang R, Zuo X, Wang K, Han Q, Zuo J, Ni H, Liu W, Bao H, Tu Y and Xie P: MicroRNA-485-5p attenuates cell proliferation in glioma by directly targeting paired box 3. Am J Cancer Res 8: 2507-2517, 2018.
18. Chai Y, Du Y, Zhang S, Xiao J, Luo Z, He F and Huang K: MicroRNA-485-5p reduces O-GlcNAcylation of Bmi-1 and inhibits colorectal cancer proliferation. Exp Cell Res 368: 111-118, 2018.
19. Hu XX, Xu XN, He BS, Sun HL, Xu T, Liu XX, Chen XX, Zeng KX, Wang SK and Pan YQ: MicroRNA-485-5p functions as a tumor suppressor in colorectal cancer cells by targeting CD147. J Cancer 9: 2603-2611, 2018.
20. Han DL, Wang LL, Zhang GF, Yang WF, Chai J, Lin HM, Fu Z and Yu JM: MiRNA-485-5p, inhibits esophageal cancer cells proliferation and invasion by down-regulating O-linked N-acetylglucosamine transferase. Eur Rev Med Pharmacol Sci 23: 2809-2816, 2019.
21. Dam DHM, Jelsma SA, Yu JM, Liu H, Kong B and Paller AS: Flotillin and AP2A1/2 promote IGF-1 receptor association with clathrin and internalization in primary human keratinocytes. J Invest Dermatol 140: 1743-1752, 2020.
22. Sonnino S and Prinetti A: Membrane domains and the 'lipid raft' concept. Curr Med Chem X20: 4-21, 2013.
23. George KS and Wu S: Lipid raft: A floating island of death or survival. Toxicol Appl Pharmacol 259: 311-319, 2012.
24. Ficht X, Ruef N, Stolp B, Samson GPB, Moalli F, Page N, Merkler D, Nichols BJ, Diz-Muñoz A, Legler DF, *et al*: In vivo function of the lipid raft protein flotillin-1 during CD8(+) T cell-mediated host surveillance. J Immunol 203: 2377-2387, 2019.
25. Lu SM and Fairn GD: Mesoscale organization of domains in the plasma membrane-beyond the lipid raft. Crit Rev Biochem Mol Biol 53: 192-207, 2018.

26. Affentranger S, Martinelli S, Hahn J, Rossy J and Niggli V: Dynamic reorganization of flotillins in chemokinestimulated human T-lymphocytes. BMC Cell Biol 12: 28, 2011.
27. Guillaume E, Comunale F, Do Khoa N, Planchon D, Bodin S and Gauthier-Rouviere C: Flotillin microdomains stabilize cadherins at cell-cell junctions. J Cell Sci 126: 5293-5304, 2013.
28. Rice T, Ishwaran H, Hofstetter W, Kelsen D, Apperson-Hansen C, Blackstone E; Worldwide Esophageal Cancer Collaboration Investigators: Recommendations for pathologic staging (pTNM) of cancer of the esophagus and esophagogastric junction for the 8th edition AJCC/UICC staging manuals. Dis Esophagus 29: 897-905, 2016.
29. Dai SL, Wei SS, Zhang C, Li XY, Liu YP, Ma M, Lv HL, Zhang Z, Zhao LM and Shan BE: MTA2 promotes the metastasis of esophageal squamous cell carcinoma via EIF4E-twist feedback loop. Cancer Sci 19: 14778, 2020.
30. Livak KJ and Schmittgen TD: Analysis of relative gene expression data using real-time quantitative PCR and the 2(-Delta Delta C(T)) method. Methods 25: 402-408, 2001.
31. Guo AY, Liang XJ, Liu RJ, Li XX, Bi W, Zhou LY, Tang CE, Yan A, Chen ZC and Zhang PF: Flotilin-1 promotes the tumorigenicity and progression of malignant phenotype in human lung adenocarcinoma. Cancer Biol Ther 18: 715-722, 2017.
32. Huang RS, Zheng YL, Li C, Ding C, Xu C and Zhao J: MicroRNA-485-5p suppresses growth and metastasis in non-small cell lung cancer cells by targeting IGF2BP2. Life Sci 199: 104-111, 2018.
33. Lee RC, Feinbaum RL and Ambros V: The C. Elegans heterochronic gene lin-4 encodes small RNAs with antisense complementarity to lin-14. Cell 75: 843-854, 1993.
34. Di Leva G, Garofalo M and Croce CM: MicroRNAs in cancer. Annu Rev Pathol 9: 287-314, 2014.
35. Chen H, Yao X, Di X, Zhang Y, Zhu H, Liu S, Chen T, Yu D and Sun X: MiR-450a-5p inhibits autophagy and enhances radiosensitivity by targeting dual-specificity phosphatase 10 in esophageal squamous cell carcinoma. Cancer Lett 28: 114-126, 2020.
36. Wang F, Li L, Piontek K, Sakaguchi M and Selaru FM: Exosome miR-335 as a novel therapeutic strategy in hepatocellular carcinoma. Hepatology 67: 940-954, 2018.
37. Qiu BQ, Lin XH, Ye XD, Huang W, Pei X, Xiong D, Long X, Zhu SQ, Lu F, Lin K, *et al*: Long non-coding RNA PSMA3-AS1 promotes malignant phenotypes of esophageal cancer by modulating the miR-101/EZH2 axis as a ceRNA. Aging (Albany NY) 12: 1843-1856, 2020.
38. Wang Y, Sun L, Wang L, Liu Z, Li Q, Yao B, Wang C, Chen T, Tu K and Liu Q: Long non-coding RNA DSCR8 acts as a molecular sponge for miR-485-5p to activate wnt/β-catenin signal pathway in hepatocellular carcinoma. Cell Death Dis 9: 851, 2018.
39. Duan J, Zhang H, Li S, Wang X, Yang H, Jiao S and Ba Y: The role of miR-485-5p/NUDT1 axis in gastric cancer. Cancer Cell Int 17: 92, 2017.
40. Gao J, Dai C, Yu X, Yin XB and Zhou F: MicroRNA-485-5p inhibits the progression of hepatocellular carcinoma through blocking the WBP2/wnt signaling pathway. Cell Signal 66: 109466, 2020.
41. Zhang Y, Hu J, Zhou W and Gao H: LncRNA FOXD2-AS1 accelerates the papillary thyroid cancer progression through regulating the miR-485-5p/KLK7 axis. J Cell Biochem 19: 1002, 2018.
42. Li G and Kong Q: LncRNA LINC00460 promotes the papillary thyroid cancer progression by regulating the LINC00460/miR-485-5p/raf1 axis. Biol Res 52: 61, 2019.
43. Bao W, Cao F, Ni S, Yang J, Li H, Su Z and Zhao B: lncRNA FLVCR1-AS1 regulates cell proliferation, migration and invasion by sponging miR-485-5p in human cholangiocarcinoma. Oncol Lett 18: 2240-2247, 2019.
44. Gao F, Wu H, Wang R, Guo Y, Zhang Z, Wang T, Zhang G, Liu C and Liu J: MicroRNA-485-5p suppresses the proliferation, migration and invasion of small cell lung cancer cells by targeting flotillin-2. Bioengineered 10: 1-12, 2019.
45. Wang FR, Xu SH, Wang BM and Wang F: MiR-485-5p inhibits metastasis and proliferation of osteosarcoma by targeting CX3CL1. Eur Rev Med Pharmacol Sci 22: 7197-7204, 2018.
46. Wang M, Cai WR, Meng R, Chi JR, Li YR, Chen AX, Yu Y and Cao XC: MiR-485-5p suppresses breast cancer progression and chemosensitivity by targeting survivin. Biochem Biophys Res Commun 501: 48-54, 2018.
47. Lin C, Wu Z, Lin X, Yu C, Shi T, Zeng Y, Wang X, Li J and Song L: Knockdown of FLOT1 impairs cell proliferation and tumorigenicity in breast cancer through upregulation of FOXO3a. Clin Cancer Res 17: 3089-3099, 2011.
48. Li Z, Yang Y, Gao Y, Wu X, Yang X, Zhu Y, Yang H, Wu L, Yang C and Song L: Elevated expression of flotillin-1 is associated with lymph node metastasis and poor prognosis in early-stage cervical cancer. Am J Cancer Res 6: 38-50, 2016.
49. Liu R, Xie H, Luo C, Chen Z, Zhou X, Xia K, Chen X, Zhou M, Cao P, Cao K and Zhou J: Identification of FLOT2 as a novel target for microRNA-34a in melanoma. J Cancer Res Clin Oncol 141: 993-1006, 2015.
50. Song L, Gong H, Lin C, Wang C, Liu L, Wu J, Li M and Li J: Flotillin-1 promotes tumor necrosis factor-alpha receptor signaling and activation of NF-κB in esophageal squamous cell carcinoma cells. Gastroenterology 143: 995-1005, 2012.
51. Jang D, Kwon H, Choi M, Lee J and Pak Y: Sumoylation of flotillin-1 promotes EMT in metastatic prostate cancer by suppressing snail degradation. Oncogene 38: 3248-3260, 2019.